Hindawi
International Journal of Polymer Science
Volume 2023, Article ID 9379277, 14 pages
https://doi.org/10.1155/2023/9379277

Research Article

Effect of *Caesalpinia decapetala* on the Dry Sliding Wear Behavior of Epoxy Composites

Hailemariam Biratu,[1] Mengistu Gelaw,[1] Kiran Shahapurkar,[1] Venkatesh Chenrayan,[1,2] Manzoore Elahi M. Soudagar,[3,4] Vineet Tirth,[5,6] Ali Algahtani,[5,6] and Tawfiq Al-Mughanam[7]

[1]*Department of Mechanical Engineering, School of Mechanical, Chemical and Materials Engineering, Adama Science and Technology University, Adama, Ethiopia 1888*
[2]*Department of Mechanical Engineering, Knowledge Institute of Technology, 637504, Salem, India*
[3]*Department of Mechanical Engineering, Graphic Era (Deemed to be University), Dehradun, Uttarakhand 248002, India*
[4]*Institute of Sustainable Energy, Universiti Tenaga National, Jalan IKRAM-UNITEN, 43000, Kajang, Selangor, Malaysia*
[5]*Mechanical Engineering Department, College of Engineering, King Khalid University, Abha 61421, Asir, Saudi Arabia*
[6]*Research Center for Advanced Materials Science (RCAMS), King Khalid University, Guraiger, Abha-61413, Asir, Saudi Arabia*
[7]*Department of Mechanical Engineering, College of Engineering, King Faisal University, P.O. Box 380, Al-Ahsa 31982, Saudi Arabia*

Correspondence should be addressed to Kiran Shahapurkar; kiranhs1588@gmail.com

Received 4 July 2023; Revised 21 September 2023; Accepted 28 September 2023; Published 25 October 2023

Academic Editor: Khubab Shaker

The present research investigates the wear characteristics of an epoxy composite reinforced with a novel *Caesalpinia decapetala* (CD) shell. The CD is available abundantly worldwide, especially in Ethiopia, particularly in East and West Oromia near West Harar. The composite specimens were processed in the open mould casting technique by varying the vol.% of CD in 10, 20, and 30. EDS is used to evaluate the important elements present in the CD. The density of composites increases with the increase in the content of CD, while the void content estimations reveal good control over the composite fabrication. The wear response of composites is investigated by varying the sliding distance and load and by maintaining a fixed velocity (5 m/s). At a 5 km slide distance and 50 N load, the 30 vol.% *Caesalpinia decapetala* composition depicts better wear resistance and friction coefficient than other compositions. Experimental results are used to envisage the ideal wear factors and to assess the influence of parameters over the two wear objectives, wear rate and CoF. The grey relational analysis- (GRA-) coupled artificial neural network (ANN) hybrid technique was employed for the prediction and validation. It has been observed that a trivial error of 0.49% amidst GRA and ANN estimation is observed.

1. Introduction

Polymer matrix composites are realized by reinforcing particulates or fibres into the polymer matrix to achieve properties better than virgin matrix [1]. Polymer matrix composites are employed in many applications ranging from small parts to big products owing to their exceptional properties [2]. Progress in developing new materials for envisaged applications is continuously rising [3]. Presently, more attention is paid to developing materials that address the application of waste materials in utilitarian composites and help reduce environmental pollution and landfill issues [4]. The effective usage of waste materials not only reduces pollution but also minimises the use of polymer, which can be considered the double benefit of utilizing waste materials [5].

Many researchers have investigated several waste materials as effective reinforcement, such as walnut shell powder [6], waste tire rubber [7], eggshell [8], fly ash cenosphere [9], rice husk [10], and blast furnace slag [11]. Particulate fillers are materials that are in powdered form, usually with a size

(a) (b)

Figure 1: *Caesalpinia decapetala* (a) seed coat and (b) plant.

less than 100 μm, and intended to reduce cost, enhance processing, and improve properties [12]. One such filler is derived from the seed shell of the *Caesalpinia decapetala* shrub found in Ethiopia [13]. This shrub is abundantly available throughout Ethiopia and is grown as a live fence and adapted to the woody grasslands and upland bushlands of western Welo, Shoa, Arsi, Harerge, and Kefa [14]. *Caesalpinia decapetala* plants are widely known for their medicinal value and are used for numerous treatments [15]. However, their despite abundant availability, they are not used for manufacturing composites. Rout and Satapathy [10] experimented with assessing the tribological performance of a rice-husk-glass-filled hybrid epoxy composite, and they employed ANN modelling to declare a significant improvement in both mechanical and tribological characteristics with the increased addition of fillers. Pattanaik et al. [16] attempted to carry out the dry sliding wear test on epoxy composite reinforced with fly ash. They utilized the TOPSIS technique to conclude that including fly ash and a normal load strongly affects the tribological property. Muralidhara et al. [17] developed a hybrid epoxy composite reinforced with carbon fibre and varying proportions of boron nitride (BN). The authors declared that the mechanical, thermal, and wear properties are significantly improved for the hybrid epoxy composite with 1% BN. Shejkar et al. [18] reported an enhancement of the physical, mechanical, and tribological properties of an epoxy composite reinforced with surface-modified wall nut shell particulates. Yadav et al. [19] attempted to develop a hybrid epoxy composite reinforced with E-glass and varying percentages of alumina up to 20%. The erosion wear report prepared through statistical analysis declared that 10% inclusion of alumina, 45° of impingement angle, 1 gm/min of discharge, and 30 m/s of impact velocity were the parameters set to minimize the erosion wear. Lohiya et al. [20] conducted an experimental examination of the epoxy composite filled with microsized Linz-Donawintz slag, and they subsequently reported that a greater improvement of mechanical and tribological properties was achieved for 40% inclusion of LD slag. Li et al. [21] prepared polytetrafluoroethylene (PTFE) particles with varying particle sizes filled with glass fibre epoxy composite to evaluate its wear resistance, and they declared that the bigger size PTFE particles had a greater influence on improving the wear resistance.

Modern manufacturing industries are experiencing greater challenges in developing a product with excellent mechanical properties and a nominal product cost. The emerging agenda for a sustainable environment and call for waste material recycling also pose a hardship on the manufacturing sector. To address the above challenges, conventional materials are being replaced with novel polymer composites reinforced with bio or synthetic waste owing to their affordable cost and abundant availability. The present research attempts to develop a wear-resistant polymer composite reinforced with biowaste *Caesalpinia decapetala* (CD) targeting the application of brake pad lining, clutch lining, centrifugal pump impeller blades, pipelines carrying mud and water mixture, and structural members in operating in an infertile environment. The CD is available in abundance worldwide, especially in Ethiopia, particularly in East and West Oromia, near West Harar. Wear rate, specific wear rate, and coefficient of friction of the composite were investigated in this study by varying the three levels of *Caesalpinia decapetala* composition (10, 20, and 30 vol.%), sliding distance of 3 and 5 km, applied load of 30, 40, and 50 N, and constant sliding velocity of 5 m/s. The hybrid GRA-ANN mathematical model has been implemented to arrive at the optimal vol.% of CD for the best wear characteristics. EDS and SEM are employed to investigate the morphological and physiochemical structure of the synthesized composite.

2. Experimental Procedure

2.1. Materials. The current study uses Lapox L-12 epoxy resin with K-6 hardener, supplied by World Glass Fiber Plc, Addis Ababa, Ethiopia, as a matrix. *Caesalpinia decapetala* seeds were collected from West Hararge, East and West Oromia regions, Ethiopia.

2.2. Caesalpinia decapetala Particulate Preparation. *Caesalpinia decapetala* were collected from the West Hararge, East and West Oromia regions, Ethiopia, as shown in Figure 1. The *Caesalpinia decapetala* seeds were separated from the

Figure 2: Processing of *Caesalpinia decapetala* seeds.

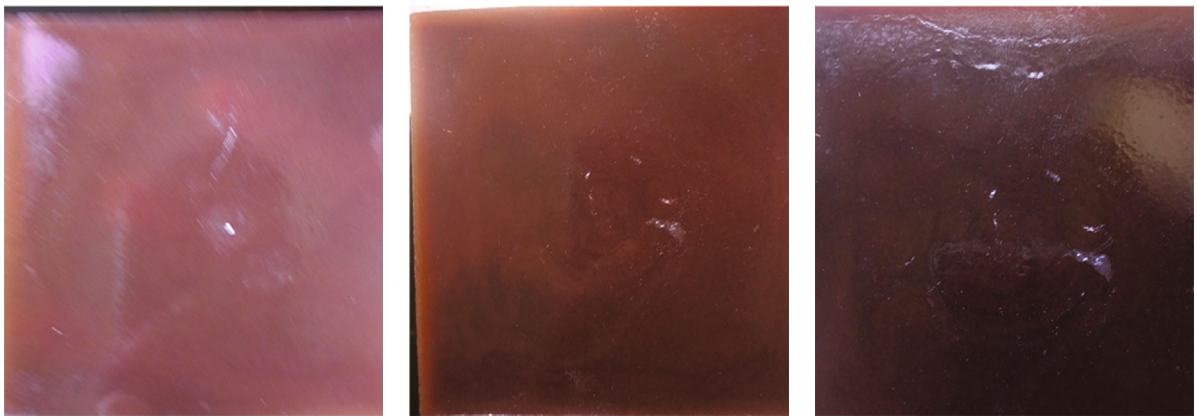

(a) (b) (c)

Figure 3: Composites with (a) 10 vol.% CD, (b) 20 vol.% CD, and (c) 30 vol.% CD.

plant and kept for drying under the sun for five days (Figure 2). Then, the manual crushing was done, followed by the complete drying in the sun. Manually crushed seeds were grounded mechanically unless they reached 75 μm. A standard 75 μm sieve filtered the fine *Caesalpinia decapetala* powder.

2.3. Composite Preparation. Four types of composites are cast using the open mould casting method by varying the *Caesalpinia decapetala* powder in 0, 10, 20, and 30 vol.%, respectively, as per the previous literature engaged with wall nut shell powder and crumb rubber powder [18, 22]. The authors reported that 20 wt.% inclusion of walnut shell powder itself agglomerated to infect the properties, while in the case of crumb rubber/epoxy composites, crumb rubber content was varied until 30 vol.%. Additionally, the authors also had trouble fabricating the composites with a higher volume percentage than 30%. Beyond 30% volume percent of CD concentration in epoxy caused severe particle aggregation and caused the composite to shatter during the polymerization process. Therefore, the addition of CD particles is restricted to 30 vol.%. The desired quantity of epoxy resin and *Caesalpinia decapetala* powder are mixed in the glass beaker with the glass rod by manual stirring. Additionally, a magnetic stirrer ensures uniform dispersion of constituents for 40 minutes. The polymerization process of the prepared slurry is instigated by adding 10 wt.% of hardener and finally decanted into a steel mould coated with silicone used as a releasing agent. Samples are alleviated for 24 hours and carefully expelled from the mould (Figure 3). The ECD-VV format indicates the specimens, wherein E pronounces epoxy matrix, CD represents *Caesalpinia decapetala*, and VV stands for volume. The rule of mixture method is followed to evaluate the theoretical density, whereas the Archimedes principle is employed to measure the experimental density by following the ASTM D792-08 standard. Cast slabs are cut as per the requirements (ASTM G99-17) using water jet machining.

2.4. Density Analyzer and Scanning Electron Microscopy. An automatic density analyzer (QUANTACHROME ULTRAPYC 1200e) is used to measure the density of CD shell

Figure 4: Dry sliding wear experimental setup [22].

Table 1: Wear factors used in the present study [26].

Input parameters		Output parameters
Caesalpinia decapetala content, (vol.%)	0, 10, 20, and 30	Wear rate (mm^3/km)
Velocity, V (m/s)	5	Specific wear rate (mm^3/km-N)
Sliding distance, D (km)	3 and 5	Coefficient of friction
Load, F (N)	30 and 50	

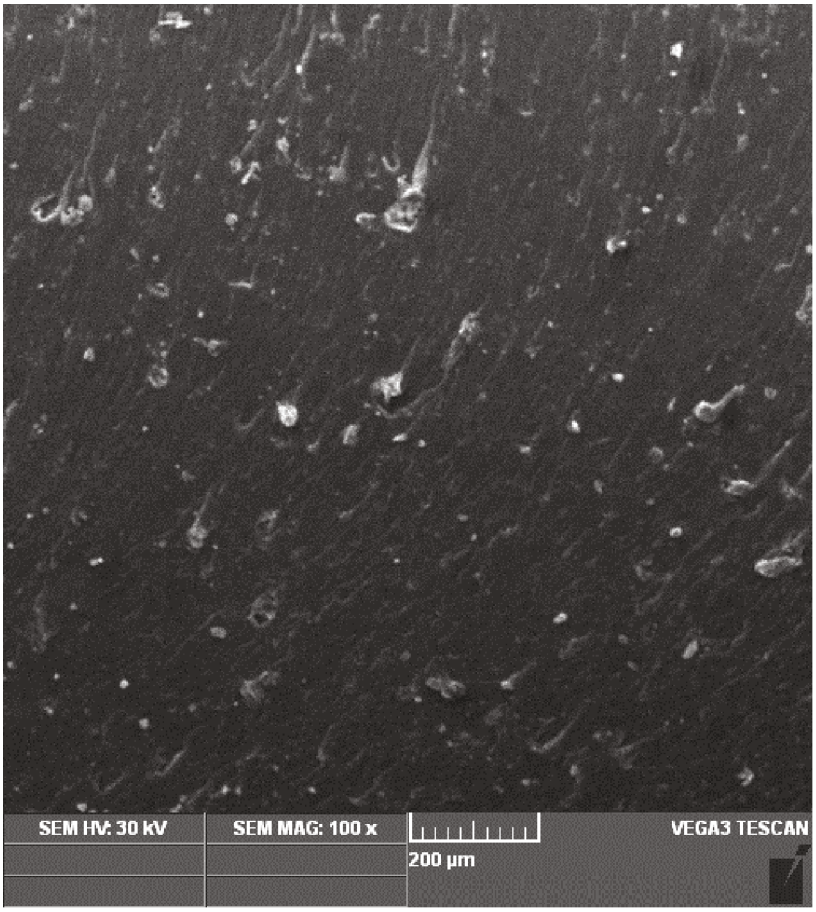

Figure 5: SEM micrograph of as-casted ECD-10 composite.

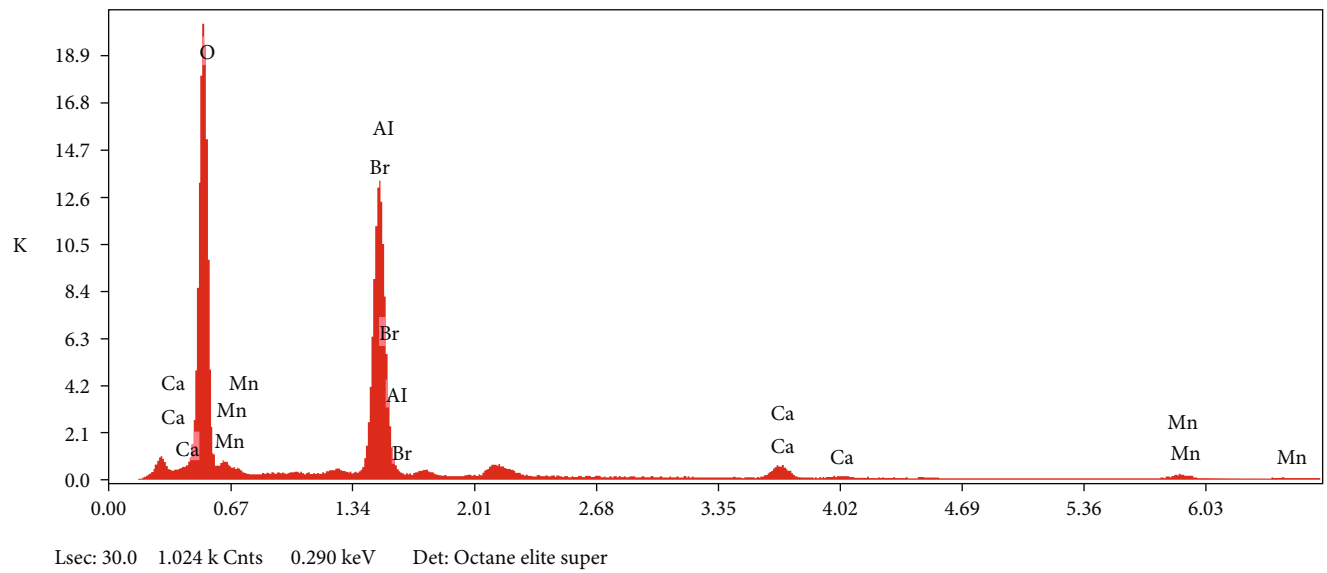

Figure 6: Energy dispersive analysis X-rays of *Caesalpinia decapetala* particles.

particles. EDS of CD powder and the surface morphology of test specimens are examined using scanning electron microscopy (JEOL JSM 6380 LA). Gold sputtering of specimens before observations is done with a JFC-1600 autofine coater, JEOL, to enhance the conductivity.

2.5. Dry Sliding Wear Test. Tests were performed using a pin-on-disc instrument purchased from DUCOM, India, as depicted in Figure 4. The wear response of the generated specimens is studied using an EN-31 disc with a 62 HRC hardness and a roughness of 0.11 μm [23]. Wear tests were done by maintaining a constant track diameter of 12 cm and 795 rpm. In Table 1, the testing parameters are listed. To imitate low and mild sliding wear conditions for brake applications, these circumstances were considered [24, 25]. Velocity, distance of sliding, and load are depicted as *Va*, *Db*, and *Fc*, respectively, wherein *a*, *b*, and *c* indicate the parametric values. The disc surface is cleaned with acetone before each test. Specimens are clamped firmly in the holder, and the tests are done, confirming ASTM G99-17. Scanning electron microscopy is utilized to evaluate the worn-out surfaces (JEOL JSM 6380 LA).

The volume loss was estimated with the help of the cross-sectional area of the pin.

Wear rate (W_r) is given as:

$$W_r = \frac{\mathrm{Vol}_e - \mathrm{Vol}_s}{\mathrm{SD}_e - \mathrm{SD}_s}, \quad (1)$$

where Vol and SD indicate the material loss in volume and distance of sliding, respectively, whereas *s* and *e* represent the before and after the experiments, correspondingly.

Specific wear rate (W_s) is given as

$$W_s = \frac{Wr}{F}. \quad (2)$$

Table 2: Chemical composition of *Caesalpinia decapetala*.

Element	Weight (%)	Atomic (%)
O K	36.93	61.23
Br K	23.23	7.71
Al K	20.69	20.34
Ca K	8.27	5.47
Mn K	10.89	5.26

Table 3: Density and void content estimations.

Composition	Theoretical density (kg/m^3)	Experimental density (kg/m^3)	Void content (%)
E	1192.00	1192.00	0.00
ECD-10	1254.60	1235.45	1.53
ECD-20	1317.20	1295.60	1.64
ECD-30	1379.80	1350.40	2.13

The coefficient of friction (CoF) (μ) is given as

$$\mu = \frac{F_t}{F_n}, \quad (3)$$

where F_t and F_n are the tangential and normal forces, respectively.

3. Results and Discussions

3.1. Physical Characterization. Figure 5 illustrates the scanning electron micrograph of ECD-10 composites that confirms the CD particles are distributed in a homogenous way. EDS spectra of *Caesalpinia decapetala* particles are presented in Figure 6. Energy peaks equivalent to the different

Table 4: Experimental observations.

S. no.	Normal load (N)	Sliding distance (km)	Percentage of composition	Sp. wear rate (mm^3/km-N)	Coefficient of friction
1	30	3	10	0.13	0.388
2	30	4	20	0.11	0.276
3	30	5	30	0.08	0.26
4	40	3	20	0.14	0.33
5	40	4	30	0.06	0.245
6	40	5	10	0.19	0.45
7	50	3	30	0.16	0.29
8	50	4	10	0.32	0.49
9	50	5	20	0.23	0.34

Table 5: S/N ratio, normalized S/N ratio, and grey coefficients.

S/N ratio		Normalized S/N ratio		Deviation sequence		Grey relational coefficient (GRC)	
Wear rate	CoF	Wear rate	CoF	(Δ_{WR})	(Δ_{CoF})	Wear rate	CoF
17.72	8.22	0.46	0.66	0.54	0.34	0.4817	0.5980
19.17	11.18	0.36	0.17	0.64	0.83	0.4395	0.3766
24.44	12.22	0.00	0.00	1.00	1.00	0.3334	0.3335
17.08	9.63	0.51	0.43	0.49	0.57	0.5032	0.4674
21.94	11.70	0.17	0.09	0.83	0.91	0.3765	0.3537
14.42	6.94	0.69	0.88	0.31	0.12	0.6164	0.8036
15.92	10.75	0.59	0.24	0.41	0.76	0.5471	0.3980
9.90	6.20	1.00	1.00	0.00	0.00	1.0004	1.0013
12.77	9.37	0.80	0.47	0.20	0.53	0.7173	0.4870

existing elements of *Caesalpinia decapetala* are depicted in tabular form (Table 2). The spectra reveal major constituents such as oxygen, bromine, aluminium, calcium, and manganese. Aluminium is an abundantly used nonferrous metal in wear-resistant applications. The presence of aluminium in the CD shell augurs for enhanced wear resistance.

The density and void estimations based on theoretical and experimental approaches are presented in Table 3. The density of composites increases with the rise in the content of *Caesalpinia decapetala*. The density of *Caesalpinia decapetala* measured using an automatic density analyzer is noted to be 1818 kg/m^3, while for epoxy, it is noted to be 1192 kg/m^3. The void content estimations are also presented in Table 3, wherein the void content increases with filler content due to small air entrapment in the composites. The void content estimations noted are very small and, therefore, can be neglected. Lower void content estimations also reveal the higher quality of composites achieved. However, the increased inclusion of CD particles increases the void content. ECD-30 reveals 2.13% of void content, which is nearly 35% more than the average void content of both CD 10 and CD 20. Hence, it is decided to curtail the inclusion of CD particles up to 30 vol.%.

3.2. Statistical Analysis

3.2.1. Taguchi's Design of the Experiment. The design of the experiment suggested by Taguchi is a unique tool to minimize the number of experiments despite the variable [27]. Since the present study involves three variable and two responses, L9 since the assessed factors are in three number and the objective are in two number, L9 orthogonal array is followed to execute the experiments [28]. Table 4 shows the sequence of experiments with their combinations of parameters and the corresponding response observations.

Table 6: Grey relational grade and their ranking.

S. no.	Grey relational grades		CGRG	Rank
	Sp. wear rate	CoF		
1	0.27	0.25	0.3716	6
2	0.32	0.25	0.4008	3
3	0.25	0.24	0.3492	9
4	0.71	0.27	0.3647	7
5	0.24	0.28	0.6928	1
6	0.25	0.25	0.3541	8
7	0.35	0.24	0.4171	2
8	0.30	0.26	0.3946	5
9	0.29	0.28	0.3968	4

3.2.2. Grey Relational Analysis (GRA). Usually, scarce data pave the way for the problems to be more complex. However, GRA presented by Ju-Long [29] could be a versatile

Table 7: Analysis of variance for wear rate.

Source	DF	Adj SS	Adj MS	F value	P value
Normal load (N)	2	0.11809	0.059045	8.58	0.104
Sliding distance (km)	2	0.01349	0.006746	0.98	0.505
Percentage of composition	2	0.18553	0.092763	13.48	0.003
Error	2	0.01377	0.006883		
Total	8	0.33087			

$R^2 = 94.84\%$; R^2 (adj) = 83.36%.

Table 8: Analysis of variance for coefficient of friction.

Source	DF	Adj SS	Adj MS	F value	P value
Normal load (N)	2	0.05589	0.027944	2.49	0.286
Sliding distance (km)	2	0.01215	0.006073	0.54	0.649
Percentage of composition	2	0.32730	0.163651	14.60	0.004
Error	2	0.02242	0.011209		
Total	8	0.41775			

$R^2 = 94.63\%$; R^2 (adj) = 88.53%.

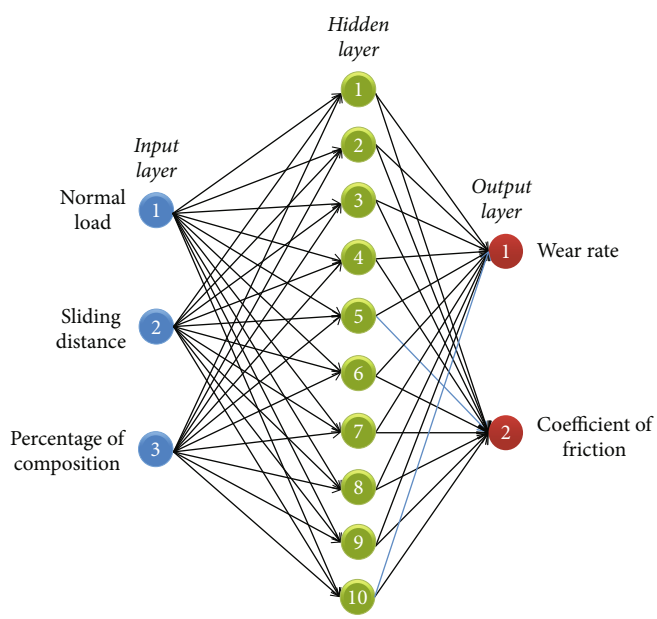

Figure 7: ANN architecture.

choice to handle these complex issues. The numerical transformation of all available data from 0 to 1, called normalizing, is a versatile way to reduce the variance in the data. This normalizing data is pivotal in transforming the multiresponse problem into a single response [30]. The variability present in the wear rate and coefficient of friction is due to unregulated variables called noise factors. The performance magnitude of the responses, whether maximum or minimum, derives the signal-to-noise ratio to reduce the effect of noise factors [31]. The current study follows the minimum the better concept; hence, the required performance magnitude of both responses is minimal. The S/N ratio arrives using the following equation to satisfy the lesser the better concept.

$$\frac{S}{N}\ \text{ratio} = -10 \log \frac{1}{n} \sum_{i=1}^{n} Y_i^2. \tag{4}$$

The normalization is being performed with the help of the following equation:

$$Z_{ij} = \frac{\max\left(Y_{ij}, i = 1, 2, \cdots, n\right) - Y_{ij}}{\max\left(Y_{ij}, i = 1, 2, \cdots, n\right) - \min\left(Y_{ij}, i = 1, 2, \cdots, n\right)}. \tag{5}$$

The inclusion of the corresponding quality loss ($\Delta_{\min}$ and $\Delta_{\max}$) function helps to arrive at an appropriate,

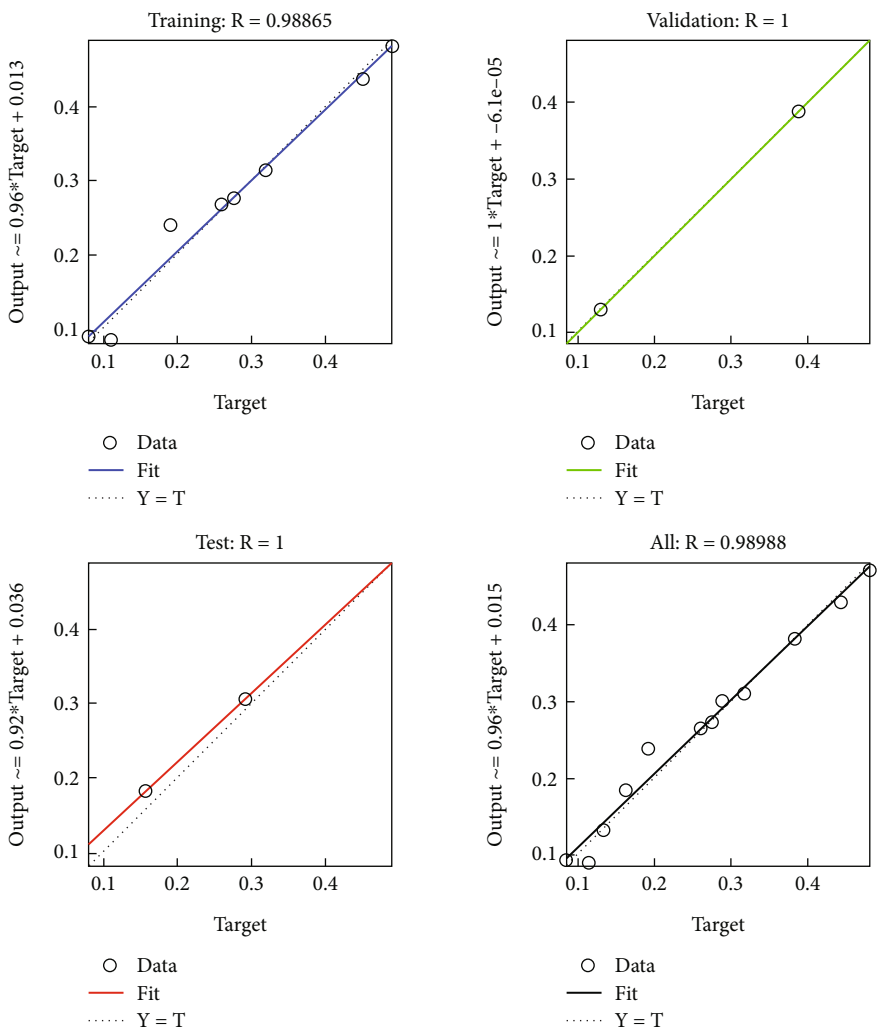

(a)

Figure 8: Continued.

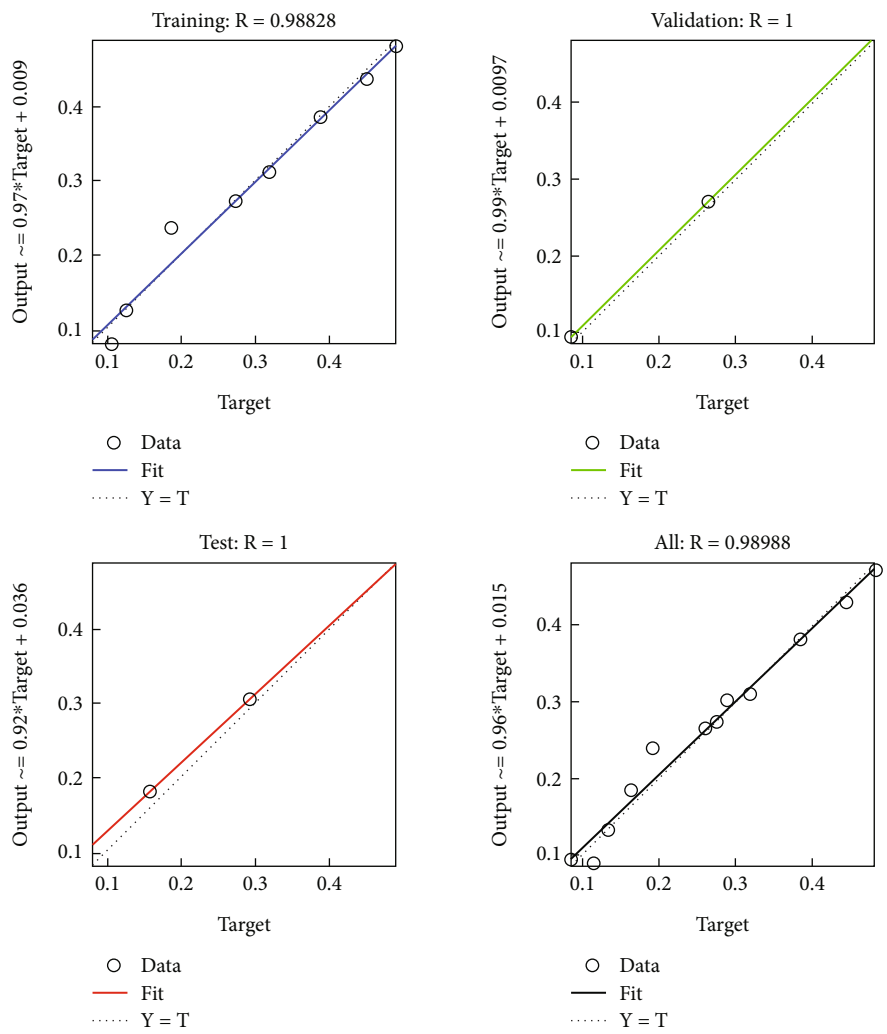

(b)

Figure 8: Prediction performance of ANN model. (a) Prediction indicator for wear rate. (b) Prediction performance for CoF.

relevant grey relational coefficient with the help of the following relation. Table 5 contains the manipulated grey relational coefficient value, S/N ratio, and normalized one.

$$GC_{ij} = \frac{\Delta_{\min} + \lambda\Delta_{\max}}{\Delta_{ij} + \lambda\Delta_{\max}}. \quad (6)$$

3.2.3. Determination of Grey Relational Grades (GRG). The following equation is used to compute the GRG [32], and their values and ranking are given in Table 6.

$$G_i = \frac{1}{m}\left(GC_{ij}\right). \quad (7)$$

where G_i is the GRG of an ith experiment and m is the number of responses.

3.2.4. Best Set of Predicted Wear Parameters. Comparing the computed GRG values helps minimize the wear characteristics indirectly. The combination of experiments with the larger value of GRG will be assigned rank no. 1. It can be seen that the wear objectives belonging to experiment no. 5, which secures the highest GRG value, are minimal. The set of wear parameters, including the wt.% inclusion of reinforcement, is declared to be an optimal wear parameter whose parameter combinations are 40 N of normal load, 4 km of sliding distance, and 30% of the composition of reinforcement.

3.2.5. Analysis of Variance (ANOVA). The objective of the study is to minimize the wear rate and coefficient of friction, which can be attained by processing the weightage of means achieved by the parameter. The mean weights are analysed through ANOVA analysis to determine the significant and insignificant parameters to induce minimum wear rate and CoF. The ANOVA table given in Tables 7 and 8 manifests the significance of the parameter through how it influences the responses. The higher value of R^2 towards unity governs the degree of suitability of the model. The higher the R^2 value, the more suitable the model. Since the P value of the percentage of composition of CD is less than 0.005 among the three wear test parameters, then the percentage of composition of CD plays a significant role in minimizing the

Table 9: Error prediction amidst experimental and ANN.

Run no.	Experimental		ANN model		Percentage of error	
	Wear rate	CoF	Wear rate	CoF	Wear rate	CoF
Training set						
1	0.13	0.388	0.12998	0.38980	0.0154	-0.4639
6	0.19	0.45	0.19000	0.45080	-0.0018	-0.1778
8	0.32	0.49	0.32005	0.48976	-0.0150	0.0490
4	0.14	0.33	0.13997	0.33040	0.0214	-0.1212
Testing set						
5	0.08	0.26	0.07989	0.25972	0.1375	0.1077
2	0.11	0.276	0.11005	0.27603	-0.0455	-0.0109
7	0.16	0.29	0.15998	0.29000	0.0125	0.0000
Validation set						
3	0.06	0.245	0.06000	0.24589	-0.0017	-0.3633
9	0.23	0.34	0.23000	0.33965	0.0009	0.1029

wear objectives. However, the normal load secured secondary importance over the objectives. The effect of sliding distance was declared insignificant when compared to the rest of the two parameters. The relationship between each parameter and the responses can be known through the regression equation given below, which is derived from the analysis.

$$\begin{aligned}\text{Wear rate} &= 0.5573 - 0.1391a_1 - 0.0586a_2 \\ &\quad + 0.1977a_3 - 0.0466b_1 + 0.0482b_2 \\ &\quad - 0.0016b_3 + 0.1422c_1 - 0.0039c_2 \\ &\quad - 0.1383c_3, \\ \text{Coefficient of friction} &= 0.5355 - 0.0994a_1 + 0.0061a_2 \\ &\quad + 0.0933a_3 - 0.0477b_1 + 0.0417b_2 \\ &\quad + 0.0059b_3 + 0.2655c_1 - 0.0918c_2 \\ &\quad - 0.1737c_3,\end{aligned} \tag{8}$$

where a_1, a_2, and a_3 are the normal load at three levels 30, 40, and 50 N, respectively; b_1, b_2, and b_3 are the sliding distance at three levels 3, 4, and 5 km, respectively; and c_1, c_2, and c_3 are the percentage of composition of CD shell powder at three levels 10, 20, and 30%, respectively.

3.3. Artificial Neural Network (ANN). The ANN is an algorithmic-based method that is versatile to handle the issues associated with modern engineering and scarce data. The neural network operating in the human biological system is the stimulating factor for developing this tool. ANN has three different processing layers: the input layer, the hidden layer, and the output later. The hidden layer employs a set of propagation functions to process the input data. The hidden layer scrutinizes the input data by using the propagation function, which is driven by the allotted weightage to the values. A certain stipulated threshold value is followed to compare the resultant value. The surpassing of the resultant value over the threshold value initiates the activation function; in turn, the outgoing weights are dispatched by the neuron to all connected neurons as an output. The algorithm regulates the allotment of weightage to the values and the activation function. The different kinds of propagation functions are utilized based on the nature of the problem. MATLAB R2018 is employed to run the ANN programme, in which the reinforcement's composition and the wear parameters are treated as input. In contrast, wear characteristics like wear rate and coefficient of friction are the output. The Levenberg-Marquardt (LM) algorithm associated with the feed-forward propagation function is used for the training. The ANN architecture shown in Figure 7 confirms the presence of one hidden layer with 10 neurons and is used to scrutinize the data. Testing is done by one out of three parts of the data, and training is done by the rest of the data.

Figures 8(a) and 8(b) depict the performance prediction of the ANN model for wear rate and CoF, respectively, and also affirm the genuineness of the prediction. The reliability of the ANN model can be realized through the collinearity of most of the points on the straight with negligible outliers. The supreme accuracy of the model is acknowledged by the R^2 value, which ranges from 0.988 to 1. The error between the experimental and the ANN can be calculated from the following equation, and Table 9 depicts the predicted error percentage.

$$\text{Percentage of error in prediction} = \frac{\text{Experimental results} - \text{ANN results}}{\text{Experimental results}} \times 100. \tag{9}$$

3.4. Wear Rate. The wear of *Caesalpinia decapetala*-reinforced epoxy composites is shown in Figure 9. Wear rates of specimens tested at constant sliding velocity (5 m/s) decrease with rising filler content and applied load. Epoxy is known to be brittle and reveals a very high wear rate [33]. Reinforcing *Caesalpinia decapetala* particles consisting of alumina as a major constituent reduces the wear rate significantly. As the *Caesalpinia decapetala* content in the composite is increased from 0 to 30 vol.%, the ability of

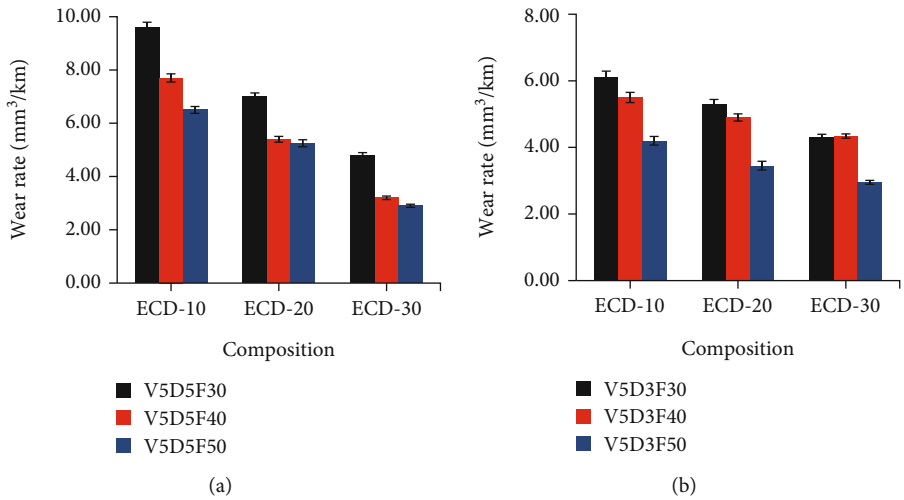

Figure 9: Wear rates of composites at sliding distances of (a) 3 and (b) 5 km.

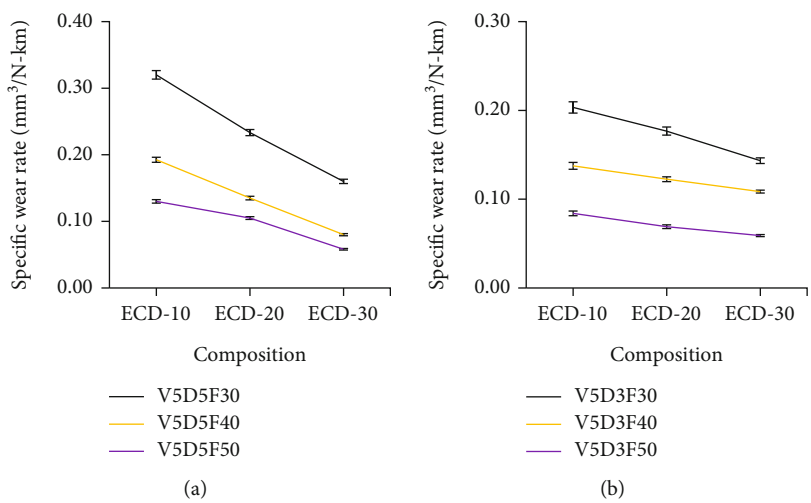

Figure 10: Specific wear rates of composites at sliding distances of (a) 3 and (b) 5 km.

composites to resist wear further enhances, and thereby the decrease in wear rate can be observed [34]. Additionally, the wear rate decreases with a rise in normal load from 30 to 50 N. Although the volume loss in epoxy-based composites depicts higher wear rates at higher applied loads, *Caesalpinia decapetala* effectively resists the wear of composites by absorbing the applied load, thereby lowering the wear rates significantly [35]. Furthermore, the reduction in brittle epoxy content compared to *Caesalpinia decapetala* content further decreases the wear rate [27]. Consequently, ECD-30 at 50 N load depicts lower wear than other compositions and test conditions which in turn upholds the results of statistical and ANN prediction. The wear rate diminished in the range of 10-35% as the applied load rose from 30 to 50 N, whereas the wear rate reduced in the range of 13-30% as the *Caesalpinia decapetala* content increased from 10 to 30 vol.%.

3.5. Specific Wear Rate. The specific wear rate of the specimens is presented in Figure 10. Similar to wear rate trends, the specific wear rates of all the composites are declining with rising applied load and *Caesalpinia decapetala* content. ECD-30 at 50 N load depicts the lowest specific wear rate of 0.059 mm^3/km-N, inferring higher wear resistance of composites.

3.6. Coefficient of Friction (CoF). The CoF of specimens subjected to different test conditions is presented in Figure 11. Irrespective of the sliding distance, CoF decreases with an increase in filler content and applied normal load. Increased *Caesalpinia decapetala* content results in lower fluctuations at the interface of the pin (specimen) and rotary disc owing to the higher resistance offered to wear by the alumina available in *Caesalpinia decapetala* particles. As a result, the surface roughness of the specimen is minimal; thereby, a low coefficient of friction is reported at higher filler loadings. Furthermore, higher applied loading also reveals a low coefficient of friction due to better compaction of asperities on the disc surface.

3.7. Postwear Analysis. Micrographs of ECD-10, ECD-20, and ECD-30 are depicted in Figures 12(a)–12(c),

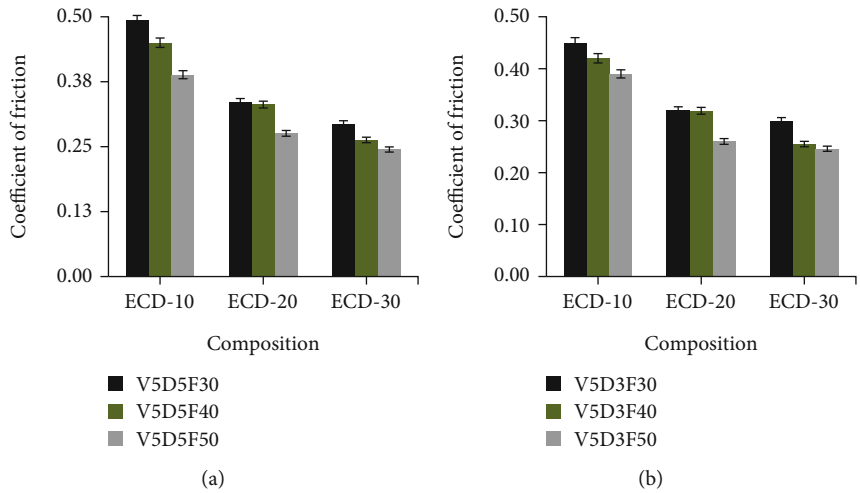

Figure 11: CoF of composites at sliding distances of (a) 3 and (b) 5 km.

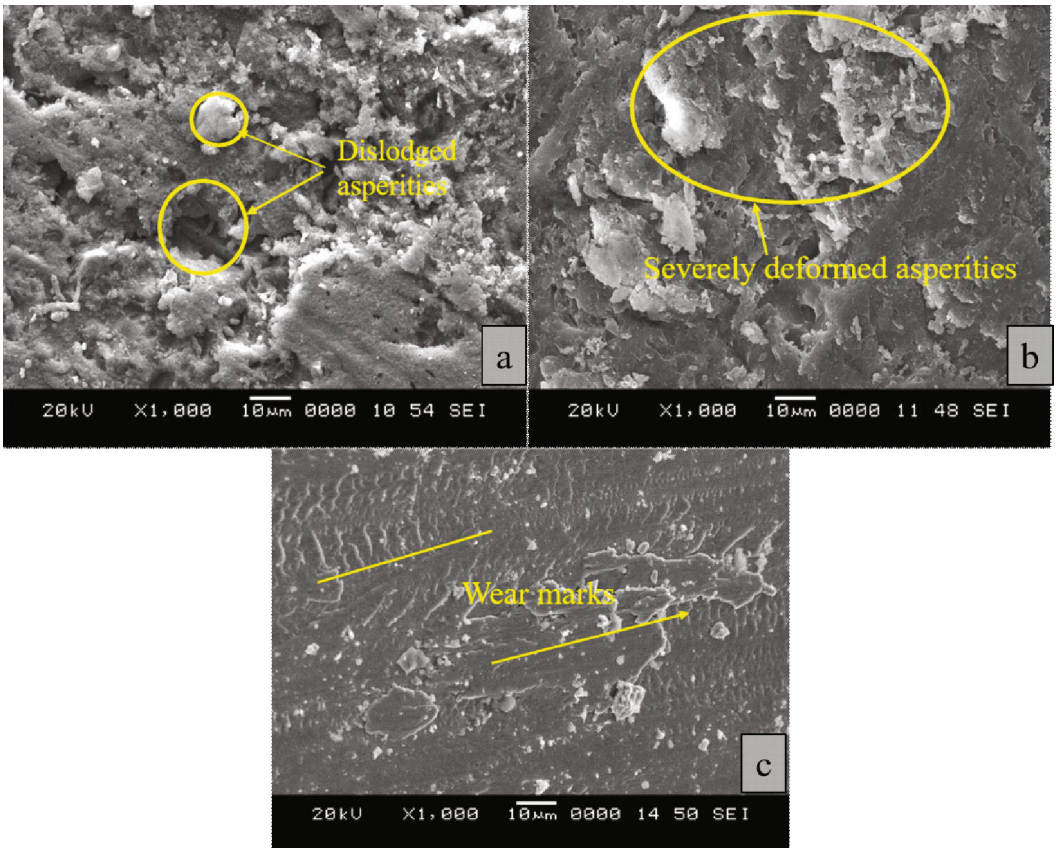

Figure 12: Scanning electron micrographs of (a) ECD-10, (b) ECD-20, and (c). ECD-30 at 50 N applied load.

respectively, postwear under the load of 50 N. The micrographs show that the wear tracks depict decreasing severity with an increase in CD shell content. Figure 12(a) manifests the dislodged asperities owing to poor resistance to the wear, which is attributed to minimal reinforcement of CD (10%). Figure 12(b) depicts the moderate wear resistance of the specimen with a 20% inclusion of CD. Still, the asperities are subjected to severe plastic deformation. Figure 12(c) confirms the enhanced wear resistance of the specimen with 30% CD inclusion, owing to the formation of a lubricant layer made out of CD particles. For the same 50 N normal load application, the specimen experiences a simple wear mark. It is found that the ceramic nature (Al_2O_3 detected by EDAX) of CD particles and their tribo-layer formation are the dominant reasons for the better wear characteristics of the specimen with an increased content of CD.

4. Conclusions

This research work comprises the development of a novel polymer composite reinforced with natural CD seed powder particulate and the assessment of the tribological behavior of the material through GRA and ANN tools. The following findings have been arrived at after rigorous analysis, and the conclusion is as follows. The addition of CD particulate improves the wear resistance capacity of the proposed composite in a versatile manner. 30 vol.% of CD particulate composite was observed to be more wear-resistant under a higher applied load. The SEM and EDS results corroborate the homogenous dispersion of reinforcement and the existence of aluminium, respectively. The natural hardness inhibited by the available ceramic content (Al_2O_3) in CD particulate was found to be the dominant reason for the improvement of wear resistance. The micrographic evaluation of worn-out surfaces manifests the tribo-layer formed by the collision of matrix materials and CD particles to hinder the interlocking of asperities. The development of a hybrid GRA-ANN analytical model estimates the best wear parameters as 40 N of normal load, 4 km of sliding distance, and 30 vol.% of the composition of reinforcement. ANOVA results obtained from GRA corroborate the importance of CD composition despite other wear parameters. R^2 value nearer to 95% assures the accuracy of the proposed model. The meagre error level of less than 0.49% between the experimental and ANN model expresses that the proposed hybrid model is suitable and adequate. The novel biowaste epoxy composite proved to be good wear-resistant; hence, the same can be recommended for functional applications like brake and clutch pad lining, pump impellers, and tiny spares exposed to water and sand slurry environments.

Data Availability

The data used to support the findings of this study are included within the article.

Conflicts of Interest

The authors declare that they have no known competing financial interests or personal relationships that could have appeared to influence the work reported in this paper.

Acknowledgments

The authors thank the Department of Mechanical Engineering, ASTU, for providing the facilities and support. The authors extend their appreciation to the Deanship of Scientific Research at King Khalid University, Abha 61421, Asir, Kingdom of Saudi Arabia, for funding this work through the Large Groups Project under grant number RGP.2/498/44. The authors acknowledge the Deanship of Scientific Research, Vice Presidency for Graduate Studies and Scientific Research at King Faisal University, Saudi Arabia, for financial support under the annual funding track (GRANT4528).

References

[1] U. S. Tewari, A. P. Harsha, A. M. Häger, and K. Friedrich, "Solid particle erosion of carbon fibre– and glass fibre–epoxy composites," *Composites Science and Technology*, vol. 63, no. 3-4, pp. 549–557, 2003.

[2] A. K. Rout and A. Satapathy, "Study on mechanical and tribo-performance of rice-husk filled glass–epoxy hybrid composites," *Materials & Design*, vol. 41, pp. 131–141, 2012.

[3] S. Devaraju, A. Hariharan, K. Balaji, and M. Alagar, "Thermal and morphological analyses of polymer matrix composites," in *Encyclopedia of Materials: Composites*, D. Brabazon, Ed., Elsevier, 2021.

[4] G. Sundararajan, M. Roy, and B. Venkataraman, "Erosion efficiency-a new parameter to characterize the dominant erosion micromechanism," *Wear*, vol. 140, no. 2, pp. 369–381, 1990.

[5] K. Soorya Prakash, P. M. Gopal, and S. Karthik, "Multi-objective optimization using Taguchi based grey relational analysis in turning of rock dust reinforced aluminum MMC," *Measurement*, vol. 157, p. 107664, 2020.

[6] S. Qi, Z. Fu, R. Yun et al., "Effects of walnut shells on friction and wear performance of eco-friendly brake friction composites," *Proceedings of the Institution of Mechanical Engineers, Part J: Journal of Engineering Tribology*, vol. 228, no. 5, pp. 511–520, 2014.

[7] S. Kunz-Douglass, P. W. R. Beaumont, and M. F. Ashby, "A model for the toughness of epoxy-rubber particulate composites," *Journal of Materials Science*, vol. 15, no. 5, pp. 1109–1123, 1980.

[8] K. Gossaye, K. Shahapurkar, V. Chenrayan et al., "Compressive behavior of Habesha eggshell particulate reinforced epoxy composites," *Polymer Composites*, vol. 44, no. 1, pp. 562–573, 2023.

[9] K. Shahapurkar, M. Doddamani, and G. C. M. Kumar, "Tensile behavior of cenosphere/epoxy syntactic foams," *AIP Conference Proceedings*, vol. 1943, no. 1, article 020100, 2018.

[10] A. Rout and A. Satapathy, "Analysis of dry sliding wear behaviour of rice husk filled epoxy composites using design of experiment and ANN," *Procedia Engineering*, vol. 38, pp. 1218–1232, 2012.

[11] Z. Wang, G. Hou, Z. Yang et al., "Influence of slag weight fraction on mechanical, thermal and tribological properties of polymer based friction materials," *Materials & Design*, vol. 90, pp. 76–83, 2016.

[12] C. DeArmitt and R. Rothon, "Particulate fillers, selection, and use in polymer composites," in *Polymers and Polymeric Composites: A Reference Series*, S. Palsule, Ed., pp. 1–26, Springer Berlin Heidelberg, Berlin, Heidelberg, 2016.

[13] R. W. Bussmann, P. Swartzinsky, A. Worede, and P. Evangelista, "Plant use in Odo-Bulu and Demaro, Bale region, Ethiopia," *Journal of Ethnobiology and Ethnomedicine*, vol. 7, no. 1, pp. 1–21, 2011.

[14] J. O. Kokwaro, *Medicinal Plants of East Africa*, East African Literature Bureau, 1976.

[15] C. M. Chaudhary, H. A. Jan, R. M. Kunwar, R. W. Bussmann, and N. Y. Paniagua-Zambrana, "*Caesalpinia decapetala (Roith) Alston Fabaceae*," in *Ethnobotany of the Himalayas*, R. M. Kunwar, H. Sher, and R. W. Bussmann, Eds., Springer International Publishing, Cham, 2020.

[16] A. Pattanaik, M. P. Satpathy, and S. C. Mishra, "Dry sliding wear behavior of epoxy fly ash composite with Taguchi optimization," *Engineering Science and Technology, an International Journal*, vol. 19, no. 2, pp. 710–716, 2016.

[17] B. Muralidhara, S. K. Babu, and B. Suresha, "Studies on mechanical, thermal and tribological properties of carbon fibre-reinforced boron nitride-filled epoxy composites," *High Performance Polymers*, vol. 32, no. 9, pp. 1061–1081, 2020.

[18] S. K. Shejkar, B. Agrawal, A. Agrawal, and G. Gupta, "Physical, mechanical, and sliding wear behavior of epoxy composites filled with surface modified walnut shell particulate," *Polymer Composites*, vol. 43, no. 10, pp. 7526–7537, 2022.

[19] R. Yadav, H.-H. Lee, A. Meena, and Y. K. Sharma, "Effect of alumina particulate and E-glass fiber reinforced epoxy composite on erosion wear behavior using Taguchi orthogonal array," *Tribology International*, vol. 175, p. 107860, 2022.

[20] P. Lohiya, A. B. Agrawal, A. Agrawal, and A. Purohit, "Physical, mechanical, and sliding wear behavior of micro-sized Linz-Donawintzslag filled epoxy composites," *Journal of Applied Polymer Science*, vol. 139, no. 31, article e52714, 2022.

[21] Z. Li, X. Qi, C. Liu, B. Fan, and X. Yang, "Particle size effect of PTFE on friction and wear properties of glass fiber reinforced epoxy resin composites," *Wear*, vol. 532-533, p. 205104, 2023.

[22] K. Shahapurkar, V. Chenrayan, M. E. M. Soudagar et al., "Leverage of environmental pollutant crump rubber on the dry sliding wear response of epoxy composites," *Polymers*, vol. 13, no. 17, p. 13, 2021.

[23] G. Straffelini and L. Maines, "The relationship between wear of semimetallic friction materials and pearlitic cast iron in dry sliding," *Wear*, vol. 307, no. 1-2, pp. 75–80, 2013.

[24] J. Bijwe, "Composites as friction materials: recent developments in non-asbestos fiber reinforced friction materials—a review," *Polymer Composites*, vol. 18, no. 3, pp. 378–396, 1997.

[25] K. Shahapurkar, V. B. Chavan, M. Doddamani, and G. C. M. Kumar, "Influence of surface modification on wear behavior of fly ash cenosphere/epoxy syntactic foam," *Wear*, vol. 414-415, pp. 327–340, 2018.

[26] M. Doddamani, G. Parande, V. Manakari, I. G. Siddhalingeshwar, V. N. Gaitonde, and N. Gupta, "Wear response of walnut-shell-reinforced epoxy composites," *Materials Performance and Characterization*, vol. 6, no. 1, article MPC20160113, 2017.

[27] A. Patnaik and A. D. Bhatt, "Mechanical and dry sliding wear characterization of epoxy–TiO2 particulate filled functionally graded composites materials using Taguchi design of experiment," *Materials & Design*, vol. 32, no. 2, pp. 615–627, 2011.

[28] C. Venkatesh and R. Venkatesan, "Optimization of process parameters of hot extrusion of SiC/Al 6061 composite using Taguchi's technique and upper bound technique," *Materials and Manufacturing Processes*, vol. 30, no. 1, pp. 85–92, 2015.

[29] D. Ju-Long, "Control problems of grey systems," *Systems & Control Letters*, vol. 1, no. 5, pp. 288–294, 1982.

[30] A. H. Suhail, N. Ismail, S. V. Wong, and N. A. A. Jalil, "Surface roughness identification using the grey relational analysis with multiple performance characteristics in turning operations," *Arabian Journal for Science and Engineering*, vol. 37, no. 4, pp. 1111–1117, 2012.

[31] S. S. Kumar, M. Uthayakumar, S. T. Kumaran et al., "Parametric optimization of wire electrical discharge machining on aluminium based composites through grey relational analysis," *Journal of Manufacturing Processes*, vol. 20, pp. 33–39, 2015.

[32] N. Kaushik and S. Singhal, "Hybrid combination of Taguchi-GRA-PCA for optimization of wear behavior in AA6063/SiCpmatrix composite," *Production & Manufacturing Research*, vol. 6, no. 1, pp. 171–189, 2018.

[33] C. Kanchanomai, N. Noraphaiphipaksa, and Y. Mutoh, "Wear characteristic of epoxy resin filled with crushed-silica particles," *Composites Part B: Engineering*, vol. 42, no. 6, pp. 1446–1452, 2011.

[34] M. G. Veena, N. M. Renukappa, B. Suresha, and K. N. Shivakumar, "Tribological and electrical properties of silica-filled epoxy nanocomposites," *Polymer Composites*, vol. 32, no. 12, pp. 2038–2050, 2011.

[35] M. Sudheer, R. Prabhu, K. Raju, and T. Bhat, "Effect of filler content on the performance of epoxy/PTW composites," *Advances in Materials Science and Engineering*, vol. 2014, Article ID 970468, 11 pages, 2014.